Modelling and Nonlinear Control of a Wet Gas Centrifugal Compressor

Torstein Thode Kristoffersen* and Christian Holden*

***Abstract*— Production of gas condensate from small and remote gas condensate fields require cost-efficient boosting technology for maintaining an economically satisfactory throughput. Wet gas compressors are a new boosting technology enabling boosting of gases containing up to 5% liquid per volume, removing the need for pre/bulk separation, resulting in lower investment and maintenance costs. However, introduction of liquid significantly changes the compression performance from that of dry gas compression, including the process gain and the normal operating region, resulting in a challenging modelling and control problem. Therefore, in this paper, we extend the commonly applied dynamic model of Greitzer for dry gas compression with one additional state and extended polynomial approximation of the compressor characteristic. A nonlinear process control algorithm, using the angular velocity as input, is derived by applying backstepping, and local asymptotic stability proven via Lyapunov analysis. The control performance is studied in different simulations with and without saturation on the control input. The steady-state performance of the dynamic model is quantitatively validated against experimental data.**

I. INTRODUCTION

Today, most of the large oil and gas discoveries in the North Sea have been developed and attention is now on smaller and more remote gas condensate fields. Development and production of these fields require cost-efficient boosting technologies and operation to achieve a sufficiently high throughput at affordable operating costs. The throughput from a producing well increases with increasing pressure difference between the well head pressure and the pressure at the receiving end (back pressure). For small fields, subsea wet gas compression is a cost-efficient boosting technology for increasing the well head pressure and thereby the well throughput to maintain an economically sufficient throughput capable of compressing gases containing up to 5% liquid per volume [1], [2], [3].

The fundamental principle of a subsea compression system is the same as that of an equivalent topside compression system, where the main difference is that a subsea compression system is designed to withstand the harsh conditions at the seabed, e.g., higher ambient pressure, corrosion, erosion, etc. [2]. Thus, results presented here can be useful for both subsea and topside facilities.

The two types of compressors most useful for gas processing are the axial and the centrifugal compressors, where the centrifugal compressor is dominant because of its high robustness and capacity [2]. The centrifugal compressor casing consists of an inducer section leading the fluid into a rotating impeller section connected to a shaft which increases the fluid velocity. The high velocity fluid leaving the impeller enters a diffuser section which decelerates the fluid resulting in an increase in fluid static pressure. The volute section is the last part of the centrifugal compressor casing and collects the decelerated fluid leaving the diffuser, leading the fluid to an exit plenum volume of much larger diameter that is equipped with a throttle [4].

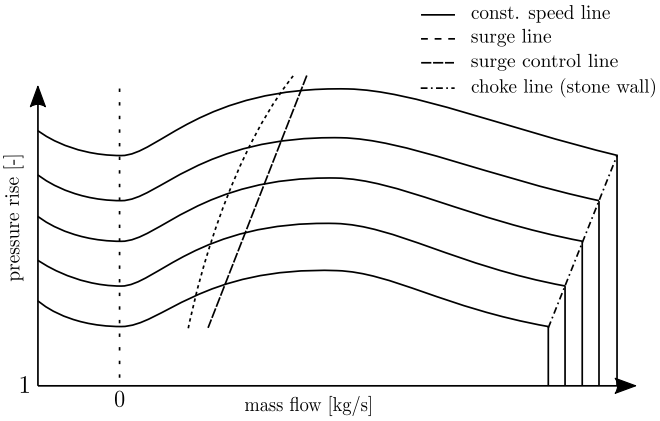

Fig. 1. A sketch of a dry gas compressor map showing the pressure ratio increase over the compressor as a function of constant rotational speed (angular velocity) including the surge line, surge control line and choke line.

The compressor performance is described by a set of curves showing the pressure rise as a function of mass flow for constant rotational speed, known as the compressor characteristic or compressor map. The compressor map is created based on measured sample points from experiments on a specific compressor. The normal operating region of the compressor map is limited by *surge* at lower mass flows and by *choke* at higher mass flows. Surge is defined as an unstable state of the compressor to the left of the stability boundary in the compressor map called the *surge line* (SL), while choke is defined as a state of the compressor at maximum mass flow.

Wet gas compression is a relatively new research area, but experiments by [5], [6] show that the compressor performance is significantly influenced by the presence of liquid. Typically, the losses increase with increasing mass flows and liquid content, resulting in reduced pressure rise for high mass flows and thereby reduced maximum capacity compared to dry gas compression. However, for low mass flows, increasing liquid content contributes to delayed instability onset as the liquid reduces the available flow area for the wet gas compression, effectively adapting the compressor for lower mass flows resulting in an increased stability region.

Dynamic modelling and control of dry gas compressors are a huge and well explored field in the literature and

* Department of Mechanical and Industrial Engineering, Norwegian University of Science and Technology (NTNU). torstein.t.k@gmail.com, christian.holden@ntnu.no

[7] provides an excellent overview. In regards to modelling and relevant for this paper, we emphasize the models of Greitzer [4] and Gravdahl and Egeland [8]. The first model describes a compression system using a set of Ordinary Differential Equations (ODEs) for describing the dynamics and an empirical 3rd order polynomial for describing the ideal pressure rise. The second model applies the same ODEs for describing the dynamics, but replaces the polynomial with an expression derived from first principles.

The most important control objective is handling surge of which there are two main strategies: active surge control (ASC) and surge avoidance (SA). *Surge avoidance* or *anti-surge control* algorithms are designed to keep the compressor operating point within the normal operating region by introducing a *surge control line* (SCL), see Fig. 1, to the right of the surge line and ensuring that the compressor operating point is kept to the right of or at this line [7]. Since the maximum pressure rise over the compressor is located at the surge line, *active surge control* algorithms have been designed to extend the normal operating region by stabilizing the unstable surge region enabling operation at the surge line [7]. A *process control* (PC) algorithm is only designed for tracking of a reference value within the normal operating region without any measures for handling or avoiding surge.

There exists a great variety of control methods for the control of *dry gas* compressors, and these mainly differ in which type of actuation and control algorithm that have been applied. This research area is too extensive to provide a complete overview in this article, and therefore, we only present short overview as a starting point for the interested reader

- control strategy/objective:
  - SA: [9], [10], [11], [12]
  - ASC: [8], [13], [14], [15], [16]
- control algorithm
  - linear: [9], [10], [12]
  - nonlinear: [8], [11], [13], [14], [15], [16]
  - MPC: [11], [12]
- control actuation/input:
  - drive torque/rotational speed: [12], [14], [15], [16]
  - throttle/recycle valve opening: [9], [10]
  - closed-coupled valve opening: [8], [11], [13]

In [13] and [16], backstepping was used to design a nonlinear surge avoidance control algorithm for a dry gas compressor.

The introduction of liquid significantly changes both the compressor performance – including the process gain and normal operating region – creating a challenging modelling and control problem. To the authors' knowledge, there exists little to no research on dynamic modelling and control of *wet gas* compressors. Therefore, in this paper, we extend the dynamic dry gas compression model of Greitzer [4] – including the corresponding compressor characteristic – with an additional state. The compressor characteristic is curve fitted to experimental data from [5]. This allows the new dynamic model to capture wet gas dynamics while maintaining a continuous transition to dry gas compression. A nonlinear process control algorithm is derived based on backstepping [17], assuming full-state feedback, and used to control the dynamic model with and without saturation on the control input. Local asymptotic stability is proven via a Lyapunov analysis.

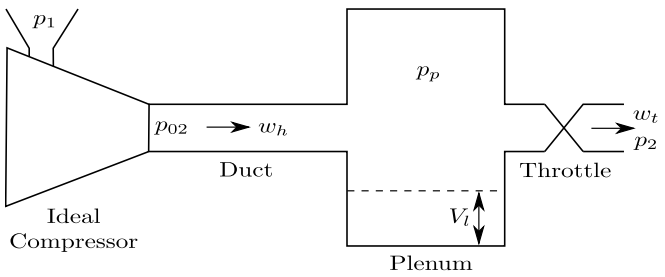

Fig. 2. A sketch of the wet gas compression system.

II. MATHEMATICAL MODEL

The compressor model, an extension of Greitzer's [4] dry gas model, is based on a simplified and idealized compression system as shown in Fig. 2. The compression system, which collectively represent the physical compressor, consists of an idealized compressor in series with a duct and a plenum volume connected with a throttle. The ideal compressor describes the ideal pressure rise over the physical compressor, while the duct describes the flow dynamics and the plenum volume describes the compression dynamics in the physical compressor. The ideal pressure rise can either be modelled physically using a first principles approach or empirically using a polynomial approximation approach [18]. We extend Greitzer's [4] dry gas model with one additional state describing the accumulation of liquid in the compressor, based on first principles, and apply an extended empirical polynomial approximation – including the inlet gas mass fraction – describing the ideal wet gas pressure rise.

A. Modelling assumptions

In order to derive the dynamic wet gas compression model, we need to make some simplifying assumptions. Similar to [4] and [8], but with the extension of considering a two-phase fluid with thermodynamic equilibrium between the phases instead of a single-phase fluid, we consider a one-dimensional two-phase fluid flow model where compressibility effects are gathered in the plenum and flow effects are gathered in the duct. According to [19], liquid will accumulate in the diffuser, resulting in an annular flow pattern and a reduced diffuser cross-sectional where fluid velocity is converted to static pressure. This observation was confirmed in experiments in [5], where an annular flow pattern was observed in the compressor, indicating separation of the flow due to the strong centrifugal forces created by the rotation of the impeller. To incorporate this wet gas effect in the model, the modelling approach of [4] is followed by dividing physical effects between different system components. Thus, we consider a homogeneously mixed flow with no separation effects in the duct and gather all separation effects in the plenum, assuming perfect separation of the duct flow as the fluid enters the plenum. The assumption of perfect separation

in the plenum allows for treating the gas and liquid in the plenum separately and thus, the gas is assumed to behave like an ideal gas. Lastly, similar to [4], losses are incorporated in the compressor characteristic and the compression process in the plenum is considered isentropic.

B. Dynamics

The polynomial approximation describing the ideal pressure rise over the compressor gives the following expression for the ideal compressor outlet pressure

$$p_{02} = \Psi(\cdot)p_1\,, \tag{1}$$

where p_1 is the inlet pressure, p_{02} is the ideal compressor outlet pressure, $\Psi(\cdot)$ is the compressor characteristic and the dot represents several arguments that later will be introduced.

The duct mass flow is derived from the momentum balance using (1) while considering an incompressible homogeneously mixed flow with no separation giving

$$\begin{aligned} \frac{\mathrm{d}}{\mathrm{d}t}\big(m_h C_h\big) &= A_d \Delta p \\ &\Downarrow \\ \frac{\mathrm{d}}{\mathrm{d}t}\Big(\big(\rho_h A_d L_d\big)\Big(\frac{w_h}{\rho_h A_d}\Big)\Big) &= (\Psi(\cdot)p_1 - p_p)A_d \\ &\Downarrow \\ \dot{w}_h = \frac{\mathrm{d}w_h}{\mathrm{d}t} &= \frac{A_d}{L_d}(\Psi(\cdot)p_1 - p_p), \end{aligned} \tag{2}$$

where m_h is the homogeneously mixed mass in the duct, w_h is the homogeneously mixed mass flow rate, C_h is the homogeneously mixed absolute velocity, ρ_h, is the homogeneously mixed density, p_p is the plenum pressure, Δp is the pressure difference over the duct, A_d is the duct cross-sectional area and L_d is the length of the duct.

As previously stated, the two-phase fluid immediately separates into separate volumes of gas and liquid as it enters the plenum. The accumulated volume of liquid reduces the available volume for gas compression leading to faster pressure dynamics and stricter requirements on control performance. The accumulated liquid volume is derived from the liquid mass balance in the plenum assuming constant liquid density

$$\begin{aligned} \frac{\mathrm{d}m_l}{\mathrm{d}t} &= (1-\beta_1)w_h - (1-\beta_p)w_t \\ &\Downarrow \\ \dot{V}_l = \frac{\mathrm{d}V_l}{\mathrm{d}t} &= \frac{1}{\rho_l}\big((1-\beta_1)w_h - (1-\beta_p)w_t\big)\,, \end{aligned} \tag{3}$$

where m_l is the liquid mass in plenum, V_l is the liquid volume in the plenum, w_t is the throttle mass flow, ρ_l is the liquid density, $\beta_1 \in (0,1]$ is the inlet gas mass fraction[1] and $\beta_p \in (0,1]$ is the plenum gas mass fraction given by

$$\beta_p = \frac{m_g}{m_g + m_l}\,, \tag{4}$$

[1]Since there is no generation (evaporation of gas or condensation of liquid) and no loss (condensation of gas or evaporation of liquid), the amount of gas and liquid in the duct remains constant, resulting in a constant gas mass fraction in the duct.

where m_g is the gas mass in the plenum.

Applying the assumptions of thermodynamic equilibrium, perfect separation in the plenum and ideal gas behaviour, the amount of gas in the plenum is given by the ideal gas law as

$$m_g = \frac{p_g M_g V_g}{R T_g} = \frac{p_p M_g (V_p - V_l)}{R T_1}\,, \tag{5}$$

where $p_g = p_p$ is the gas pressure in the plenum equal to the plenum pressure, M_g is the gas molar mass, V_g is the volume of gas in the plenum, V_p is the plenum volume, R is the ideal gas constant and $T_g = T_1$ is the gas temperature in the plenum equal to the homogeneous mixed fluid temperature due to the thermodynamic equilibrium assumption.

The amount of liquid in the plenum is given by the definition of density as

$$m_l = \rho_l V_l\,. \tag{6}$$

An alternative expression for the plenum gas mass fraction is obtained by substituting (5) and (6) into (4) giving

$$\beta_p = \frac{p_p M_g (V_p - V_l)}{p_p M_g (V_p - V_l) + \rho_l R T_1 V_l}\,. \tag{7}$$

The plenum pressure, representing the accumulated amount of gas in the plenum, is derived from the gas mass balance in the plenum assuming ideal gas behaviour with perfect separation as

$$\begin{aligned} \frac{\mathrm{d}m_g}{\mathrm{d}t} &= \beta_1 w_h - \beta_p w_t \\ &\Downarrow \\ V_g \frac{\mathrm{d}\rho_g}{\mathrm{d}t} + \rho_g \frac{\mathrm{d}V_g}{\mathrm{d}t} &= \beta_1 w_h - \beta_p w_t \\ &\Downarrow \\ \frac{\mathrm{d}\rho_g}{\mathrm{d}t} &= \frac{1}{V_p - V_l}\Big(\beta_1 w_h - \beta_p w_t + \rho_g \frac{\mathrm{d}V_l}{\mathrm{d}t}\Big)\,, \end{aligned} \tag{8}$$

where ρ_g is the gas density. For isentropic compression of ideal gases, the following relation between gas density and gas pressure holds [18]

$$\mathrm{d}\rho_g = \frac{1}{c_g^2}\mathrm{d}p_g = \frac{1}{c_g^2}\mathrm{d}p_p\,, \tag{9}$$

where $c_g = \sqrt{\gamma R T_1 / M_g}$ is the dry gas speed of sound and γ is the specific dry gas heat capacity ratio. The plenum pressure dynamics is obtained by substituting (3) and (9) into (8) giving

$$\begin{aligned} \dot{p}_p = \frac{\mathrm{d}p_p}{\mathrm{d}t} = \frac{c_g^2}{V_p - V_l}\Big(&\beta_1 w_h - \beta_p w_t \\ &+ \frac{p_p M_g}{R T_1 \rho_l}\Big((1-\beta_1)w_h - (1-\beta_p)w_t\Big)\Big)\,. \end{aligned} \tag{10}$$

To complete the dynamic model, we need an algebraic expression for the throttle outlet flow. The fluid leaving the plenum is assumed to instantaneously mix homogeneously and density of this homogeneous mixture is given by [5]

$$\rho_p = \frac{\rho_g \rho_l}{\beta_p \rho_l + (1-\beta_p)\rho_g}\,. \tag{11}$$

The throttle flow is given by the valve equation using (11)

$$w_t = k_t \sqrt{\rho_p (p_p - p_2)}\,, \tag{12}$$

where p_2 is the back pressure and k_t is an empirical throttle constant.

C. Static pressure rise

In literature, a 3rd-order polynomial as a function of mass flow and rotational speed is commonly used to approximate dry gas compressor characteristics [4], [15], [18]. The reason for this is that the pressure rise typically has the shape of a 3rd-order function as illustrated in Fig. 1. For dry gas compression the gas mass fraction is constant and therefore not included in the polynomial approximation. However, for wet gas compression the gas mass fraction is changing and therefore must be included in the polynomial approximation. Since the experimental wet gas compressor map [5] only includes the normal operating region, i.e., the mass flows between surge and choke, a 2nd-order polynomial provides sufficient accuracy, see Fig. 3. Applying a 3rd-order polynomial is possible if more data is considered. We therefore use a 2nd-order polynomial of three variables, i.e., mass flow, inlet gas mass fraction and rotational speed, to approximate the compressor characteristic.

The 2nd-order polynomial approximation of the compressor characteristic is then given by

$$\begin{aligned}\Psi(w_h, \beta_1, \omega) = c_0 + c_1 w_h + c_2 \beta_1 + c_3 \omega + c_4 w_h^2 + c_5 w_h \beta_1 \\ + c_6 w_h \omega + c_7 \beta_1^2 + c_8 \beta_1 \omega + c_9 \omega^2\,,\end{aligned} \tag{13}$$

where c_i is the ith constant coefficient and ω is the angular velocity of the drive shaft.

For calculating the coefficients of the 2nd-order polynomial, we apply the method of nonlinear least squares using the Matlab function `lsqcurvefit` [20]. The polynomial approximation is curve-fitted to the wet gas compressor characteristic obtained from [5]. The resulting polynomial is shown in Fig. 3 and the calculated coefficients and residual in Table I. As the figure shows and the residual indicates, the 2nd-order polynomial provides a quite accurate approximation of the experimentally obtained curves. The polynomial approximation is not valid outside this normal operating region.

D. Model summary

The ordinary dynamic equations (ODEs) describing the dynamic wet gas compressor model is summarized below

$$\begin{aligned}\dot{p}_p = \frac{c_g^2}{V_p - V_l}\Big(&\beta_1 w_h - \beta_p w_t \\ &+ \frac{p_p M_g}{R T_1 \rho_l}\Big((1-\beta_1) w_h - (1-\beta_p) w_t\Big)\Big)\end{aligned} \tag{14}$$

$$\dot{w}_h = \frac{A_d}{L_d}\big(\Psi(w_h, \beta_1, \omega) p_1 - p_p\big) \tag{15}$$

$$\dot{V}_l = \frac{1}{\rho_l}\big((1-\beta_1) w_h - (1-\beta_p) w_t\big)\,. \tag{16}$$

The wet gas compressor model reduces to the dry gas compressor model with $\beta_1 = \beta_p = 1$.

TABLE I

CALCULATED 2ND-ORDER POLYNOMIAL COEFFICIENTS AND RESIDUAL.

Polynomial coefficients	2nd-order polynomial
c_0	$5.1757 \cdot 10^{-1}$
c_1	$-2.8779 \cdot 10^{-1}$
c_2	$7.0458 \cdot 10^{-2}$
c_3	$1.0501 \cdot 10^{-3}$
c_4	$-2.8873 \cdot 10^{-1}$
c_5	$1.4441 \cdot 10^{-1}$
c_6	$4.7954 \cdot 10^{-4}$
c_7	$-9.5474 \cdot 10^{-2}$
c_8	$1.0259 \cdot 10^{-4}$
c_9	$-3.4193 \cdot 10^{-7}$
Residual	$4.3844 \cdot 10^{-3}$

III. CONTROL DESIGN

The design of the backstepping process control algorithm is based on general theory from [17] with full-state knowledge of the plant using ω as control input.

A. Assumptions

To derive a backstepping control algorithm adapted for use in industrial applications we make the simplifying assumption of a constant liquid volume in the plenum, implying that $\beta_p = \beta_1$ and $w_t(p_p, V_l) = w_t(p_p)$. Additionally, we assume that the constant liquid volume is less than the plenum volume, i.e., $V_p > V_l$, and that the back pressure is smaller than the inlet pressure, i.e., $p_1 > p_2$. Thus, the simplified system is given by

$$\dot{x}_1 = f_1(V_l) f_2(\beta_1, x_1)\Big(x_2 - w_t\Big) \tag{17}$$

$$\dot{x}_2 = k_2\Big(\Psi(x_2, \beta_1, u) p_1 - x_1\Big) \tag{18}$$

where $x = [x_1, x_2]^\top = [p_p, w_h]^\top$ is the simplified system states, $u{=}\omega$ is the input and V_l is a constant, $k_1 = RT_1 > 0$ and $k_2 = \frac{A_d}{L_d} > 0$ are constants and $f_1(V_l) = \frac{c_g^2}{V_p - V_l} > 0$ and $f_2(\beta_1, x_1) = \beta_1 + \frac{M_g x_1}{k_1 \rho_l}(1-\beta_1) > 0$. To simplify the backstepping design, the aggregated input

$$v = \Psi(x_2, \beta_1, u) p_1\,, \tag{19}$$

is considered as the input to the simplified system.

The objective of the surge avoidance control algorithm is to have the plenum pressure $x_1 = p_p$ track the constant reference p_{ref}.

B. Stabilization by backstepping

To apply theory from [17], the origin of (17) is shifted so that the plenum pressure reference becomes the origin of the transformed system. The control objective is to achieve asymptotic tracking of p_{ref} for the transformed system.

The backstepping method starts by designing a stabilizing control input for the output state using the subsequent state as virtual input and then recursively follows this procedure until the actual input is used for design of the stabilizing control input. For the simplified system (17),(18), the plenum

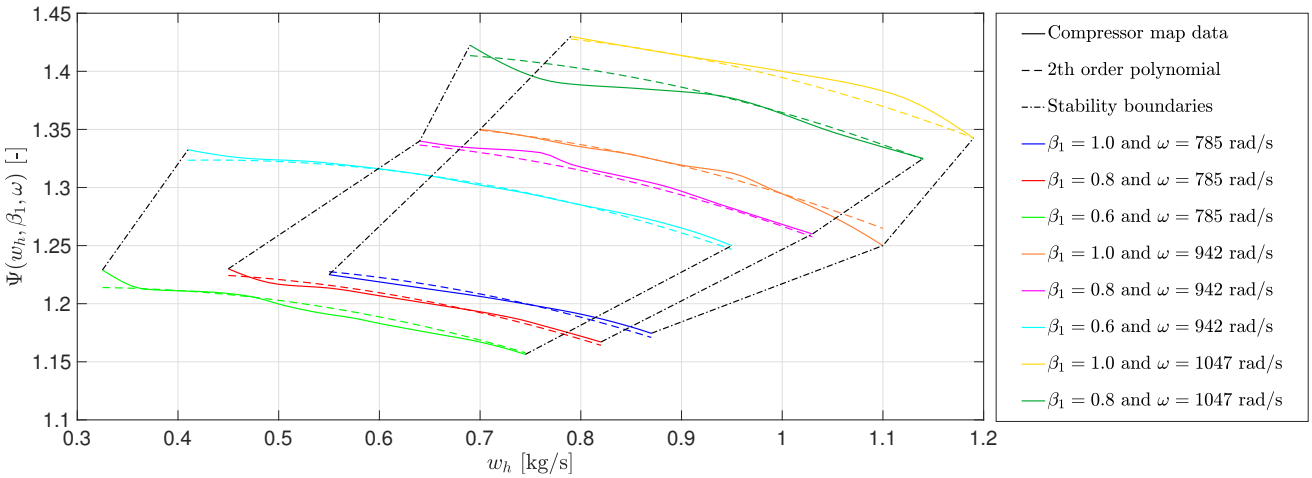

Fig. 3. Experimental compressor map (solid) [5] vs. polynomial approximation (dashed) for various gas mass fractions.

pressure x_1 is the output state, the mass flow x_2 is the virtual input and v is the actual input.

The following theorem can now be stated:

Theorem 1. *Assume that $p_{\text{ref}} \geq p_2 + \epsilon$ and $\epsilon > 0$. Then, the equilibrium point $x^\top = [p_{\text{ref}}, w_t(p_{\text{ref}})]$ of the system (17)–(18) is locally asymptotically stable with the control input*

$$\begin{aligned} v &= \Psi(x_2, \beta_1, u) p_1 \\ &= -\frac{1}{d_2 k_2}\Big[k_{p2}\big(x_2 - w_t\big) - k_{p1}k_{p2}\big(x_1 - p_{\text{ref}}\big) - d_2 k_2 x_1 - \dot{w}_t \\ &\quad + f_1(V_l) f_2(\beta_1, p_{\text{ref}})\Big(d_1\big(x_1 - p_{\text{ref}}\big) + d_2 k_{p1}\big(x_2 - w_t\big)\Big)\Big], \end{aligned} \tag{20}$$

where d_1, $d_2 > 0$ are positive constants and $k_{p1} > 1$ and $k_{p2} > 0$ are positive gains.

Proof. The proof is divided into two recursive steps by the backstepping method.

1) Step 1 – stabilization of x_1 using x_2 as virtual input: For the first recursive design step, we shift the origin of (17) to the plenum pressure reference and stabilize this transformed state using x_2 as a virtual input. Hence, the first backstepping variable (error variable) is defined as

$$z_1 = x_1 - p_{\text{ref}}\,. \tag{21}$$

The resulting z_1-subsystem is given by

$$\dot{z}_1 = f_1(V_l) f_2(\beta_1, z_1 + p_{\text{ref}})\Big(x_2 - w_t\Big). \tag{22}$$

The virtual input is defined as

$$x_2 = z_2 + \lambda\,, \tag{23}$$

where z_2 is the second backstepping variable and λ is a stabilizing function we can choose to stabilize the z_1-subsystem.

We choose the positive definite Lyapunov function candidate for design of the stabilizing virtual input as

$$V_1(z_1) = \frac{1}{2} d_1 z_1^2\,, \tag{24}$$

where d_1 is a positive constant. The time derivative of V_1 along the trajectories of the system (22) is given by

$$\dot{V}_1(z_1) = d_1 f_1(V_l) f_2(\beta_1, z_1 + p_{\text{ref}})\Big(z_1 z_2 + (\lambda - w_t) z_1\Big), \tag{25}$$

where (23) has been inserted. Since x_2 is considered as virtual input for the z_1-subsystem, the z_2-terms are ignored for this design step (cross terms are considered in the next design step).

In order to make $\dot{V}_1(z_1)$ negative definite in z_1, the following stabilizing function is chosen:

$$\lambda = w_t - k_{p1} z_1 \tag{26}$$

where the first term has been included for cancelling of the nonlinear dynamics and the second term with the positive constant k_{p1} has been added for stabilizing of the z_1-subsystem.

Inserting (26) into (25) gives

$$\dot{V}_1(z_1) = -d_1 f_1(V_l) f_2(\beta_1, p_{\text{ref}})\Big(k_{p1} z_1^2 - z_1 z_2\Big) + \text{H.O.T.} \tag{27}$$

Since $f_2(\beta_1, p_{\text{ref}})$ is linear in its second argument and positive, $\dot{V}_1(z_1)$ is negative definite for small z_1 and $z_2 = 0$. Thus, the z_1-subsystem is locally stabilized with x_2 as virtual input.

2) Step 2 – stabilization of x_2 using v as actual input: The origin of (18) is shifted by the stabilizing function (26). For the second recursive design step, we stabilize this transformed state using the actual input v. The z_2-subsystem is given by

$$\begin{aligned} \dot{z}_2 &= k_2\Big(v - (z_1 + p_{\text{ref}})\Big) - \dot{w}_t \\ &\quad + f_1(V_l) f_2(\beta_1, z_1 + p_{\text{ref}})\Big(k_{p1} z_2 - k_{p1}^2 z_1\Big). \end{aligned} \tag{28}$$

We choose the positive definite Lyapunov function candidate for design of the stabilizing actual input

$$V_2(z) = V_1(z_1) + \frac{1}{2} d_2 z_2^2\,, \tag{29}$$

where d_2 is a positive constant. The time derivative of V_2 along the trajectories of (22) and (28) with λ given by (26) gives

$$\begin{aligned} \dot{V}_2(z) &= -d_1 f_1(V_l) f_2(\beta_1, z_1 + p_{\text{ref}})\Big[k_{p1} z_1^2 - z_1 z_2\Big] \\ &\quad + d_2 f_1(V_l) f_2(\beta_1, z_1 + p_{\text{ref}})\Big[k_{p1} z_2^2 - k_{p1}^2 z_1 z_2\Big] \\ &\quad + d_2 z_2\Big[k_2 v - k_2(z_1 + p_{\text{ref}}) - \dot{w}_t\Big] \end{aligned}$$

$$
\begin{aligned}
=&-d_1 f_1(V_l) f_2(\beta_1, p_{\text{ref}}) k_{p1} z_1^2 \\
&+z_2\Big[f_1(V_l) f_2(\beta_1, p_{\text{ref}})\Big(d_1 z_1 + d_2 k_{p1} z_2 \\
&-d_2 k_{p1}^2 z_1\Big)+d_2 k_2\Big(v-(z_1+p_{\text{ref}})\Big)-\dot{w}_t\Big]+\text{H.O.T.}
\end{aligned} \tag{30}
$$

In order to make $\dot{V}_2(z)$ negative definite in $z^\top = [z_1, z_2]$, the following actual input is chosen

$$
\begin{aligned}
v = -\frac{1}{d_2 k_2}\Big[&f_1(V_l) f_2(\beta_1, p_{\text{ref}})\Big(d_1 z_1 + d_2 k_{p1} z_2 \\
&- d_2 k_{p1}^2 z_1\Big)-d_2 k_2\big(z_1 + p_{\text{ref}}\big)-\dot{w}_t + k_{p2} z_2\Big],
\end{aligned} \tag{31}
$$

where the first terms have been included for cancelling the nonlinear dynamics and the last term with the positive constant k_{p2} has been added for stabilizing the z_2-subsystem.

Inserting (31) into (30) gives

$$
\dot{V}_2(z) = -d_1 f_1(V_l) f_2(\beta_1, p_{\text{ref}}) k_{p1} z_1^2 - k_{p2} z_2^2 + \text{H.O.T.} \tag{32}
$$

which is negative definite for small z, assuming $\dot{w}_t$ exists and is well-defined. In the appendix, we derive the exact expression for $\dot{w}_t$ and prove that it exists and is well-defined if $p_{\text{ref}} \geq p_2 + \epsilon$ for $\epsilon > 0$.

Thus, by [17, Theorem 4.1], the origin of the z-system is locally asymptotically stable. From (21) and (26), we see that the $x \to z$ map is a diffeomorphism. The point $x^\top = [p_{\text{ref}}, w_t(p_{\text{ref}})]$ corresponds to the point $z = 0$, and thus the point $x^\top = [p_{\text{ref}}, w_t(p_{\text{ref}})]$ is locally asymptotically stable. □

The preceding proof only holds for $v = \Psi(x_2, \beta_1, u) p_1$ as the control input, however in reality $u = \omega$ is the actual control input. For calculating the actual control input using the control law stated in Theorem 1, we solve the optimization problem

$$
u = \arg \min_{\underline{u} \leq u \leq \overline{u}} \Big(v - \Psi(x_2, \beta_1, u) p_1\Big)^2, \tag{33}
$$

where $\overline{u}$ and $\underline{u}$ are the maximum and minimum angular velocity that the wet gas compressor is able to deliver, as specified by the compressor characteristic in Fig. 3.

Because of the simple nature of $\Psi(u; x_2, \beta_1)$, (33) can be solved explicitly. To find the inverse of $\Psi(x_2, \beta_1, u)$ with respect to u, the following function is defined

$$
\tilde{\Psi}(\tilde{u}\,; x_2, \beta_1) = \Psi(x_2, \beta_1, \tilde{u}) = A\tilde{u}^2 + B\tilde{u} + C\,, \tag{34}
$$

where A, B and C are given by

$$
A = c_9 \tag{35}
$$

$$
B(x_2, \beta_1) = c_3 + c_6 x_2 + c_8 \beta_1 \tag{36}
$$

$$
C(x_2, \beta_1) = c_0 + c_1 x_2 + c_2 \beta_1 + c_4 x_2^2 + c_5 x_2 \beta_1 + c_7 \beta_1^2\,. \tag{37}
$$

The inverse of $\tilde{\Psi}(\tilde{u}\,; x_2, \beta_1)$ is derived from the quadratic formula and the relation $\tilde{\Psi}(\tilde{u}\,; x_2, \beta_1) = v/p_1$

$$
\tilde{u} = \tilde{\Psi}^{-1}(v/p_1; x_2, \beta_1) = -\frac{B}{2A} \pm \sqrt{\Big(\frac{B}{2A}\Big)^2 - \frac{C - (v/p_1)}{A}}. \tag{38}
$$

The 2nd-order polynomial approximation $\Psi(x_2, \beta_1, u)$ has only one solution as seen in Fig. 3. Since the solution of (38) with a positive quadratic term has no physical interpretation, as it only generates angular velocities far above what the compressor is able to produce, the following solution of (38) is chosen

$$
\tilde{u} = -\frac{B}{2A} - \sqrt{\Big(\frac{B}{2A}\Big)^2 - \frac{C - (v/p_1)}{A}}. \tag{39}
$$

Complex roots correspond to u being saturated. Therefore, we introduce constraints on the control law to account for limited control inputs and avoid complex control inputs. The constrained control law is given by

$$
u = \begin{cases} \overline{u} & \text{Re}(\tilde{u}) \geq \overline{u} \\ \text{Re}(\tilde{u}) & \underline{u} < \text{Re}(\tilde{u}) < \overline{u} \\ \underline{u} & \text{Re}(\tilde{u}) \leq \underline{u} \end{cases}. \tag{40}
$$

IV. SIMULATIONS

The nonlinear process control laws (31) and (40) are studied in three different simulation scenarios for the actual plant (14)–(16). In Scenario 1, β_1 varies while p_{ref} is constant. In Scenario 2, β_1 is constant while p_{ref} changes, and in Scenario 3, both β_1 and p_{ref} change. Simulation results are shown in Figs. 4–6 where blue curves are the results from using u, orange curves are the results from using v and the black curve is the inlet conditions and control input limits that are the

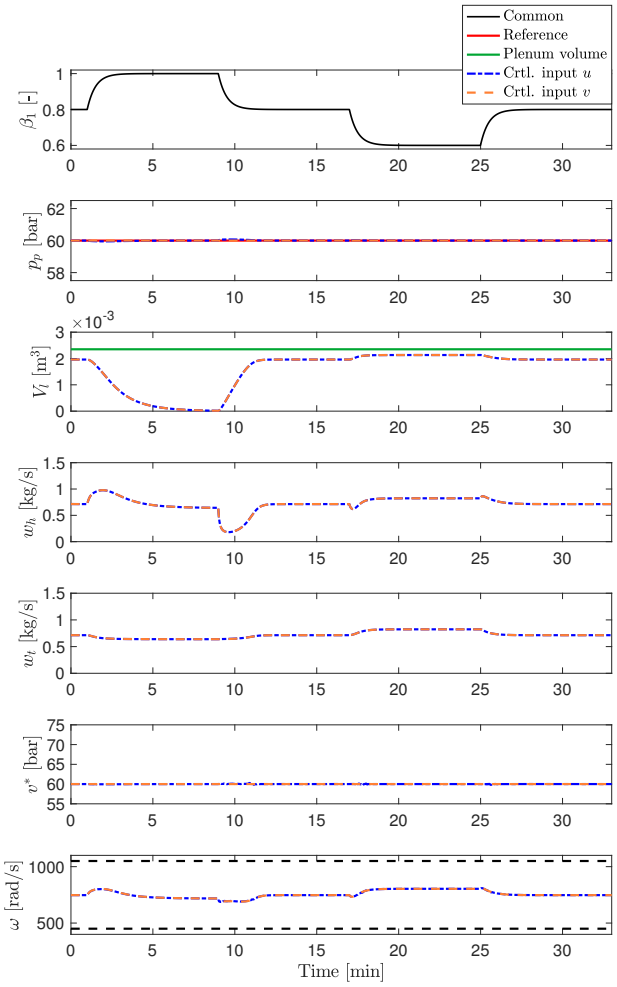

Fig. 4. Transient response for Scenario 1 where the label Common refers to inlet conditions or control input limits that are common for both nonlinear control laws. The labels Ctrl. input v and Ctrl. input u represent the control response for the different nonlinear control laws.

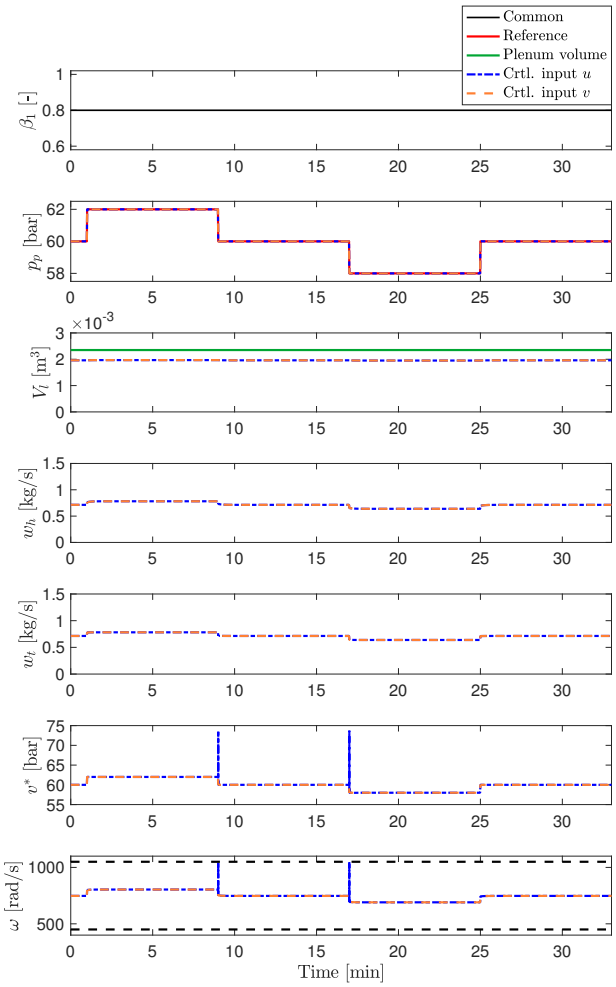

Fig. 5. Transient response for Scenario 2 where the label Common refers to inlet conditions or control input limits that are common for both nonlinear control laws. The labels Ctrl. input v and Ctrl. input u represent the control response for the different nonlinear control laws.

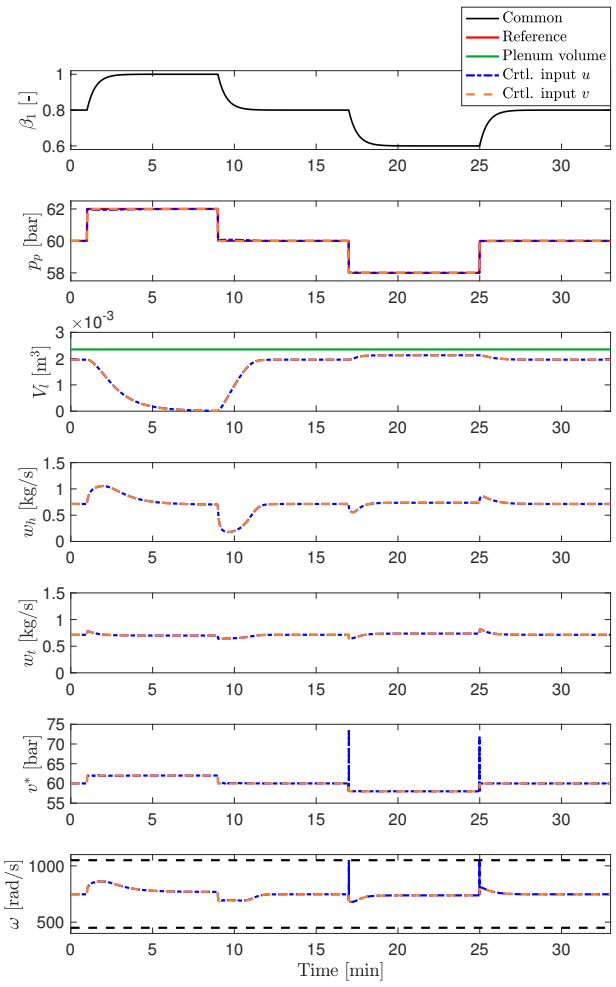

Fig. 6. Transient response for Scenario 3 where the label Common refers to inlet conditions or control input limits that are common for both nonlinear control laws. The labels Ctrl. input v and Ctrl. input u represent the control response for the different nonlinear control laws.

same for both control algorithms. The simulation and tuning parameters used in the simulations are given in Table II.

As one control algorithm has input v in Pa and the other u in rad/s, the control input from each of the nonlinear control algorithms are converted to the matching converted control input form to enable comparison. Thus, for the nonlinear control laws v and u the control input is converted to angular velocity $u^* = \tilde{\Psi}^{-1}(v/p_1\,; x_2, \beta_1)$ and aggregated input $v^* = \Psi(x_2, \beta_1, u)p_1$, respectively. The asterisks signs represent converted control inputs.

For all the simulation scenarios, both nonlinear process control laws are able to control the pressure without oscillations or offset. As expected, all variables behave equally for both nonlinear process control laws with the exception of a few transients for the control input variable. These transients occur upon infinitely fast, step changes in the control reference causing u to generate complex control inputs that are constrained, while v handles these transients smoothly.

TABLE II

SIMULATION AND TUNING PARAMETERS.

ρ_g [kg/m^3]	ρ_l	c_g [m/s]	M_g [kg/mole]	k_1 [J/mole]	k_2 [m]	k_t [m^2]	k_{p1} [m s]	k_{p2} [s]	d_1 [m^{2}s^2]	d_2 [-]
3.33	1000	300	28.96	2685	5.83	0.004	15	20	1	1000

Note that the nonlinear process control laws were derived assuming a constant accumulated liquid volume and constant parameters (β_1, p_1, T_1), and that local stability was only proven for this case. However, the simulations were performed with a non-constant accumulated liquid volume and a time-varying inlet gas mass fraction; despite of this, the control laws were able to control the process.

The simulations show that the plenum volume occupied by the gas drastically reduces, compared to the plenum volume occupied by the liquid, for increasing liquid content. This behaviour is due to the homogeneously mixed flow assumption, causing the accumulated liquid volume to change such that the plenum gas mass fraction (4) equals the inlet gas mass fraction at steady-state. The reduced plenum volume available for gas compression results in faster pressure dynamics, i.e., the pressure transient response for wet gas compression is faster compared to that of dry gas compression. However, the steep pressure change subsequent to the step change in the pressure reference, occurring each eight minutes, is only made possible by the nonlinear control algorithm. Uncontrolled, the pressure would rapidly diverge.

V. CONCLUSIONS AND FURTHER WORK

A dynamic model of a wet gas compressor with an empirical polynomial describing the compressor characteristic was derived from first principles, and the empirical polynomial was curve-fitted to a wet gas compressor map obtained from previously published experiments. A nonlinear process control law with the pressure rise as control input was derived using backstepping, and locally asymptotic stability of the reference point was proven using Lyapunov analysis. This control law was, without any stability proof, extended with the angular velocity as control input. The control laws were compared in simulations.

The dynamic part of the model was derived from first principles providing physical insight and a wide range of validity, while the compressor characteristic is empirical providing no physical insight and is only valid for a specific compressor unit. Only the steady-states of the model, i.e., the ideal pressure rise, is validated against experimental data and experimental validation of the dynamic response is future work. The wet gas compressor characteristic is described using a 2nd-order polynomial approximation providing validity for a specific wet gas compressor unit. A wet gas compressor characteristic derived from first principles would provide a wider range of validity and valuable insight into wet gas compression, and is future work.

The control laws with the pressure rise and the angular velocity as control input were able to control the actual plant without oscillations or offset in the controlled pressure variable. The control laws achieved control of the actual plant with moderate control input usage. However, upon infinitely fast, step changes in the control reference, the control law with the angular velocity as the control input generates spikes in the control input that are confined by the constraints, while the control law with the pressure rise as the control input handles these changes smoothly without spikes.

The derived control laws use the pressure rise as control input, while the actual control input is the angular velocity. There is a static mapping between these control inputs and as long as this mapping is invertible, there exists a smooth mapping between these control inputs. As shown in simulations, this mapping exists in almost all situations. Simulations show that more aggressive tuning and/or smoother steps remove the exceptions, but a formal proof is future work.

The control laws are derived assuming a constant liquid volume in plenum and constant parameters, while the actual liquid volume is non-constant and the parameters are time-varying. In simulations, the changing liquid volume and the time-varying inlet gas mass fraction did not hamper the efficiency of the nonlinear control laws; the plenum pressure still converges to the desired value. However, a formal proof remains future work.

APPENDIX

A. Existence and uniqueness of $\dot{w}_t$

The throttle flow w_t of (17),(18) is given by

$$w_t(x_1) = k_t\sqrt{\rho_1(x_1 - p_2)} = k_t\sqrt{\rho_1(z_1 + p_{\text{ref}} - p_2)}\,, \quad (41)$$

where ρ_1 is the inlet homogeneously mixed flow density. The time derivative of the simplified throttle flow is given by

$$\dot{w}_t = \frac{k_t\rho_1}{2\sqrt{\rho_1(x_1 - p_2)}}\dot{x}_1 = \frac{k_t\rho_1}{2\sqrt{\rho_1(z_1 + p_{\text{ref}} - p_2)}}\dot{x}_1. \quad (42)$$

If $p_{\text{ref}} \geq p_2 + \epsilon$ and $\epsilon > 0$, then w_t and $\dot{w}_t$ (and here $\dot{x}_1$, which contains w_t) exists and are well-defined for $z_1 > -\epsilon$, which contains the z-origin.

ACKNOWLEDGMENTS

This project is supported by the Norwegian Research Council, NTNU and industrial partners under the Subsea Production and Processing (SUBPRO) SFI program.

REFERENCES

[1] R. Fantoft, "Subsea gas compression - challenges and solutions," in *Offshore Technology Conference*, 2005.

[2] L. Brenne, T. Bjørge, L. E. Bakken, and Ø. Hundseid, "Prospects for sub sea wet gas compression," in *Proceedings of the AMSE Turbo Expo 2008: Power for land, sea and air*, 2008.

[3] O. Økland, S. Davies, R. M. Ramberg, and H. Rognø, "Steps to the subsea factory," in *Offshore Technology Conference*, 2013.

[4] E. M. Greitzer, "Surge and rotating stall in axial flow compressors - part I: Theoretical compression system model," *Journal of Engineering for Power*, 1976.

[5] T. G. Grüner and L. E. Bakken, "Wet gas impeller test facility," in *Proceedings of the ASME Turbo Expo 2010: Power for land, sea and air*, 2010.

[6] ——, "Instability characteristic of a single-stage centrifugal compressor exposed to dry and wet gas," in *Proceedings of the ASME Turbo Expo 2012: Power for land, sea and air*, 2012.

[7] F. Willems and B. de Jager, "Modeling and control of rotating stall and surge: An overview," in *Proceedings of the IEEE International Conference on Control Applications*, 1998.

[8] J. T. Gravdahl and O. Egeland, "Centrifugal compressor surge and speed control," in *IEEE Transactions on Control Systems Technology*, 1999.

[9] O. O. Badmus, C. N. Nett, and F. J. Schork, "An integrated, full-range surge control/rotating stall avoidance compressor control system," in *Proceedings of the American Control Conference*, 1991.

[10] K. M. Murphy, P. Kalata, R. Fischl, and D. Marchio, "On modeling surge avoidance control (SAC) in compressors: desgin procedure," in *Proceedings of the American Control Conference*, 1995.

[11] T. A. Johansen, "On multi-parametric nonlinear programming and explicit nonlinear model predictive control," in *Proceedings of the 41st Conference on Decision and Control*, 2002.

[12] A. Cortinovis, H. J. Ferreau, D. Lewandowski, and M. Mercangöz, "Safe and efficient operation of centrifugal compressors using linearized MPC," in *Proceedings of the 53rd Conference on Decision and Control*, 2014.

[13] J. T. Gravdahl and O. Egeland, "Compressor surge control using a close-coupled valve and backsteeping," in *Proceedings of the American Control Conference*, 1997.

[14] J. T. Gravdahl, F. Willems, and O. E. Bram de Jager, "Modeling for surge control of centrifugal compressors: comparison with experiment," in *Proceedings of the 39th IEEE Conference on Decision and Control*, 2000.

[15] J. T. Gravdahl, O. Egeland, and S. O. Vatland, "Active surge control of centrifugal compressors using drive torque," in *Proceedings of the 40th IEEE Conference on Decision and Control*, 2001.

[16] B. Bøhagen and J. T. Gravdahl, "Active surge control of compression system using drive torque," *Automatica*, 2008.

[17] H. K. Khalil, *Nonlinear Systems*. Prentice-Hall, 1996.

[18] O. Egeland and J. T. Gravdahl, *Modeling and Simulation for Automatic Control*. Marine Cybernetics, 2002.

[19] L. Brenne, "Straight-walled diffuser performance," Ph.D. dissertation, Norwegian University of Science and Technology (NTNU), 2004.

[20] L. Ljung, *System Identification: Theory for the user*. Prentice Hall, 2006.